Hysteretic properties of a magnetic particle with strong surface anisotropy

H. Kachkachi* and M. Dimian

Laboratoire de Magnétisme et d'Optique, Université de Versailles St. Quentin, 45 av. des Etats-Unis, 78035 Versailles, France

(Received 1 October 2001; revised manuscript received 11 February 2002; published 11 November 2002)

We study the influence of surface anisotropy on the zero-temperature hysteretic properties of a small single-domain ferromagnetic particle, and investigate limiting cases where deviations from the Stoner-Wohlfarth model are observed due to nonuniform reversal of the particle's magnetization. We consider a spherical particle with simple cubic crystal structure, a uniaxial anisotropy for core spins, and radial anisotropy on the surface. The hysteresis loop is obtained by solving the local (coupled) Landau-Lifshitz equations for classical spin vectors. We find that when the surface anisotropy constant K_s assumes large values, e.g., of the order of the exchange coupling J, large deviations are observed with respect to the Stoner-Wohlfarth model in the hysteresis loop and thereby the limit-of-metastability curve, since in this case the magnetization reverses its direction in a nonuniform manner via a progressive switching of spin clusters. This characteristic value of K_s depends on the surface-to-volume ratio of exchange coupling and the angle between the applied field and core easy axis.

DOI: 10.1103/PhysRevB.66.174419 PACS number(s): 75.50.Tt, 75.70.Rf, 75.10.Hk

I. INTRODUCTION

Surface effects have a strong bearing on the properties of small magnetic systems, and entail large deviations from the bulk behavior. It was shown in Ref. 1 that the magnetic disorder on the surface caused by surface anisotropy is long ranged, which implies that even the spins in the core of a very small magnetic particle (2 nm) render a magnetization that deviates from the bulk value. It will be useful to understand surface effects in magnetic materials in order to control their properties which are relevant for technological applications. One such property is the coercive field as it gives indications on the relaxation time of the magnetization and thereby on the stability of the information stored on magnetic media.

Surface effects are due to the breaking of crystal-field symmetry, and this is a local effect. So, in order to study such effects one has to resort to microscopic theories, unlike the macroscopic Stoner-Wohlfarth (SW) model,[2] which are capable of distinguishing between different atomic environments and taking account of physical parameters such as bulk and surface anisotropy, exchange, and dipole-dipole interactions. Unfortunately, this leads to difficult many-body problems which can only be dealt with using numerical approaches.

This work deals with the effect of strong surface anisotropy on the hysteretic properties (hysteresis loop and limit-of-metastability curve, the so-called SW astroid), of a single-domain spherical particle (with free surfaces), a simple cubic (sc) crystal structure, a uniaxial anisotropy in the core, and radial single-site anisotropy for spins on the boundary. The hysteresis loop and thereby the critical field are computed by solving, at zero temperature, the local Landau-Lifshitz equations derived from the classical anisotropic Dirac-Heisenberg model in field, subjected to a local condition (see below) accounting for the minimization of energy with respect to local rotations of each spin in the particle. In Ref. 3 the same method was used for studying the hysteretic properties of models of nanoparticles, where the anisotropy was either random in the whole particle or taken only on the surface, and the analysis was restricted to the hysteresis loop.

In this paper, we use an improved version of the method mentioned above including a global-rotation condition on the resultant magnetic moment of the particle in addition to the local condition (see Ref. 4). We compute the hysteresis loop and infer from it the limit-of-metastability curve (SW astroid), and compare with the SW model especially when the surface anisotropy constant assumes large values, e.g., $K_s/J \sim 1$. This study has allowed us to investigate the limit of validity of the SW model for very small magnetic particles where surface anisotropy plays a determinant role, and whose magnetization no longer switches in a coherent way.

Our method, based on the numerical solution of the Landau-Lifshitz equation at zero temperature, is checked against the SW semianalytical results in two limiting cases of the exchange coupling with different distributions of anisotropy axes. We first consider a single-domain particle with a macroscopic magnetic moment resulting from very strong exchange interaction. This is equivalent to the SW one-spin problem with uniaxial anisotropy. A second test deals with the case of a square particle of noninteracting spins all with randomly distributed easy axes. This model mimics an assembly of monodispersed single-domain nanoparticles with a random distribution of their easy axes embedded in a two-dimensional (2D) nonmagnetic matrix.

The plan of this work is as follows: we first define our model (Hamiltonian and physical parameters), present the method used for computing the hysteresis loop, and test it against the semianalytical results of SW model. Then, we discuss our results for a spherical particle in terms of exchange coupling, particle's size, and surface anisotropy by varying, in turn, one of them while keeping the other two fixed. We also study the situation with (intra)surface exchange coupling different from that in the core of the particle. A short account of the present work can be found in Ref. 5. It is worth mentioning though that in fact only anisotropy and exchange coupling on the surface can be considered as free parameters as there are so far no definite experimental estimations thereof.

II. MODEL HAMILTONIAN

We consider the following classical anisotropic Dirac-Heisenberg model:

$$\mathcal{H}=-\sum_{\langle i,j\rangle} J_{ij}\mathbf{S}_i\cdot\mathbf{S}_j-(g\mu_B)\mathbf{H}\cdot\sum_{i=1}^{\mathcal{N}}\mathbf{S}_i+H_{an}, \tag{1}$$

where $\mathbf{S}_i$ is the unit spin vector on site i, $\mathbf{H}$ is the uniform magnetic field applied in a direction ψ with respect to the reference z axis, $\mathcal{N}$ is the total number of spins (core and surface), and in the sequel D will denote the particle's diameter. $J_{ij}(=J>0)$ is the strength of the nearest-neighbor exchange interaction, which will be taken in our calculations the same everywhere inside the particle, unless otherwise specified (see Fig. 14 *et seq.*); H_{an} is the uniaxial anisotropy energy,

$$H_{an}=-\sum_i K_i(\mathbf{S}_i\cdot\mathbf{e}_i)^2, \tag{2}$$

with easy axis $\mathbf{e}_i$ and constant $K_i>0$. This anisotropy term contains either of the two contributions stemming from the core and surface, and depends on the system under consideration. For instance, for the 2D model (which serves as a test of our calculations by comparison with the SW model) all spins (core and surface) have the same anisotropy constant but randomly distributed axes. In the case of a spherical particle, all core spins are attributed the same constant K_c and all surface spins are attributed the constant K_s. Moreover, core spins will have an easy axis along the z axis, whereas a surface spin is assumed to have its anisotropy axis along the radial direction, see Ref. 6 and many references therein.

A more physically appealing microscopic model of surface anisotropy was provided by Néel,[7]

$$H_{an}^{Neel}=-K_s\sum_i\sum_{j=1}^{z_i}(\mathbf{S}_i\cdot\mathbf{e}_{ij})^2, \tag{3}$$

where z_i is the coordination number of site i and $\mathbf{e}_{ij}=\mathbf{r}_{ij}/r_{ij}$ is the unit vector connecting the site i to its nearest neighbors. This model is more realistic since the anisotropy at a given site occurs only when the latter loses some of its neighbors, i.e., when it is located on the boundary. However, the extra sum on nearest neighbors in Eq. (3) makes this model less practical for numerical calculations, especially those that are time consuming, such as the SW astroid. So in this paper we restrict ourselves to the model of radial single-site anisotropy on the surface. In Ref. 8, we have developed an analytical theory, together with the numerical method used here, for weak surface anisotropy and studied this model and compared it with the radial-anisotropy model.

A remark is in order concerning the dipole-dipole interactions inside the particle. It is well known[9] that these relativistic interactions lead to two contributions, a first term that is an integral over the volume of the particle, and a second one over the surface. The latter represents the magnetostatic energy. However, it has been shown[10] that in very small particles the first contribution is negligible as compared with the contribution of exchange interactions. On the other hand, the second contribution plays the role of shape anisotropy, which for a spherical particle yields an irrelevant constant. Therefore in our case of very small spherical particles, where the effect of surface anisotropy constant is most important, which is one of the main issues of the present work, the volume term is negligible and the shape anisotropy is absent.

III. METHOD OF CALCULATION OF THE HYSTERESIS LOOP

Different models of a nanoparticle are studied. In each case, we simulate the lattice with sc crystal structure, and then assign to each site a length-fixed three-component spin vector. For the calculation of the hysteresis loop we start with a magnetic configuration where all spins are pointing in the same direction $-z$, which corresponds to the saturation state. The hysteresis loop is due to the existence of metastable states in the system. Starting from the initial configuration and applied field, the integration of the Landau-Lifshitz equation (see below) tends towards a new configuration that is an energy minimum.

Let us now establish the Landau-Lifshitz equations for the magnetic moments. We choose K_c as the energy scale and normalize the other physical constants accordingly, i.e.,

$$t\rightarrow\frac{2K_c}{\hbar}\times t,\quad \mathbf{h}\equiv\frac{(g\mu_B)}{2K_c}\times\mathbf{H}. \tag{4}$$

Then, the Landau-Lifshitz (LL) equation for a spin $\mathbf{S}_i$ at site i, reads

$$\frac{d\mathbf{S}_i}{dt}=-\mathbf{S}_i\times\mathbf{h}_i^{eff}-\alpha\mathbf{S}_i\times(\mathbf{S}_i\times\mathbf{h}_i^{eff}), \tag{5}$$

where $\alpha(\sim 1)$ is the damping parameter and $\mathbf{h}_i^{eff}$ is the effective field acting on the spin $\mathbf{S}_i$ and is given by

$$\mathbf{h}_i^{eff}=\mathbf{h}+\frac{1}{2K_c}\sum_{j=1}^{z_i}J_{ij}\mathbf{S}_j+\mathbf{h}_i^{an}, \tag{6}$$

where $\mathbf{h}_i^{an}\equiv-(\partial H_{an}/\partial\mathbf{S}_i)/2K_c$, with H_{an} given in Eq. (2), z_i is the coordination number of site i. In the sequel, we will use the reduced parameters, $j\equiv J/K_c$, $k_s\equiv K_s/K_c$. Therefore for each site i we arrive at three coupled equations (for S_i^x, S_i^y, S_i^z), and because of the second term in Eq. (6) we actually obtain a system of $3\mathcal{N}$ (local) coupled equations. We emphasize that it is more convenient to use spherical coordinates (for each spin) instead of the Cartesian ones. Indeed, owing to the fact that the spins are of constant length, this reduces the number of individual (for each spin) equations to 2 instead of 3,

$$\dot{\theta}_i=(h_\varphi^{eff}+\alpha h_\theta^{eff})_i, \tag{7}$$

$$\dot{\varphi}_i=(-h_\theta^{eff}+\alpha h_\varphi^{eff})_i/\sin\theta_i,$$

where $h_\theta^{eff}\equiv-\partial\mathcal{H}/\partial\theta, h_\varphi^{eff}\equiv-\partial\mathcal{H}/\partial\varphi$ are the polar components of the effective field. For the one-spin problem, these are obtained by direct differentiation of the energy written in

spherical coordinates, whereas for a particle it is not possible to obtain a tractable analytical expression of the energy in spherical coordinates, so h_θ^{eff} and h_φ^{eff} are written in terms of the time derivatives of the Cartesian components of $\mathbf{h}_i^{eff}$ in Eq. (6). Using Eq. (7) instead of Eq. (5) allows for a gain of computer time, but this method encounters stability problems specific to the spherical coordinates, because of the factor $1/\sin\theta$ in Eq. (7), which diverges as $\theta \to 0, \pi$, and hence a special care is required when numerically handling these equations.

After having constructed the magnetic structure (lattice and spin vectors on it), we apply a magnetic field **H** at some angle ψ with respect to the reference z axis, with values chosen in a regular mesh. Then we calculate the local effective field for all spins and thereby the right-hand sides of the LL equations (7) and proceed with the time integration. As this is done, the total energy in Eq. (1) smoothly decreases, and some criterion must be used for stopping the integration for the given value of the applied field and moving to the next value. In our calculations we proceed to the next field value when

$$\frac{1}{\mathcal{N}} \sum_{i=1}^{\mathcal{N}} \left| \frac{d\mathbf{S}_i}{dt} \right| < \varepsilon, \tag{8}$$

which implies that the system is close to a stationary state, ε being a small parameter of the order of 10^{-5}–10^{-7}. However, it was shown in Ref. 4, that this local condition, which accounts for the minimization of energy with respect to local rotations (or small deviations) of each spin, must be supplemented by a global condition on the resultant magnetic moment so as to account for the global rotation of the particle's magnetic moment. Obviously, for a single spin these two conditions boil down to one and the same condition (8).

Next, the stationary state thus obtained is used as the initial state for the next value of the field. Iteration of this process over a sequence of applied fields, of given magnitude and direction ψ, renders the hysteresis loop. For each value of this angle we determine the critical or switching field (see discussion below). The whole procedure finally renders the critical or switching field as a function of the angle ψ, which in the case of critical field is the SW astroid.

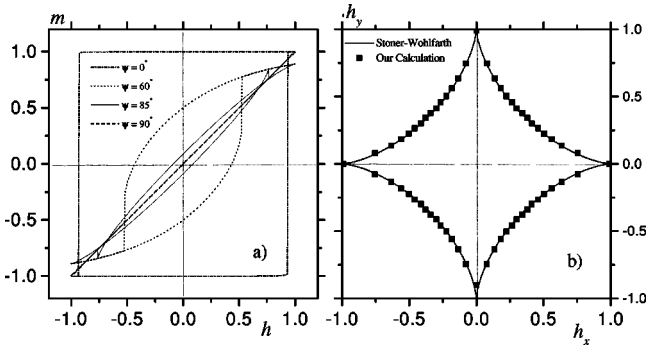

FIG. 1. Left: (numerical) hysteresis loops for different values of ψ increasing inwards: ψ=0,60°,85°,90°, for a 3^3 particle with uniaxial anisotropy. For the sake of clarity the SW analytical hysteresis loops have been omitted, since they exactly coincide with the computed ones. Right: (numerical in squares and analytical in full line) SW astroid for the same particle; $j=10$.

As a test of this method, we considered a box-shaped particle with[11] $\mathcal{N}=3^3$, a sc structure, uniaxial anisotropy, and strong exchange interaction between spins inside the particle, and computed the hysteresis loop for different values of the angle ψ between the applied field and the easy axis. The results are shown in Fig. 1 (left). Next, we present in Fig. 1 (right) the SW astroid, which separates the region with two minima of energy from that with only one minimum. We see that the SW results are exactly reproduced by our calculations. We have also computed the hysteresis loop of a square particle of noninteracting spins ($J=0$) all with randomly distributed easy axes. This is equivalent to an assembly of monodispersed single-domain noninteracting particles with randomly distributed easy axes in two dimensions. As expected, we find that the remanent magnetization is equal to 1/2.

For later reference, we plot in Fig. 2 the critical field h_c and the height of the magnetization jump (i.e., $m_u - m_d$), as functions of the angle ψ between the direction of the field and core easy axis. Obviously, $h_c(\psi)$ in Fig. 2 (left) is a well-known result of the Stoner-Wohlfarth model.

On the other hand, we note that the height of magnetization jump has an almost linear dependence on ψ, except for the final portion $76° < \psi < 90°$, which corresponds to cycles

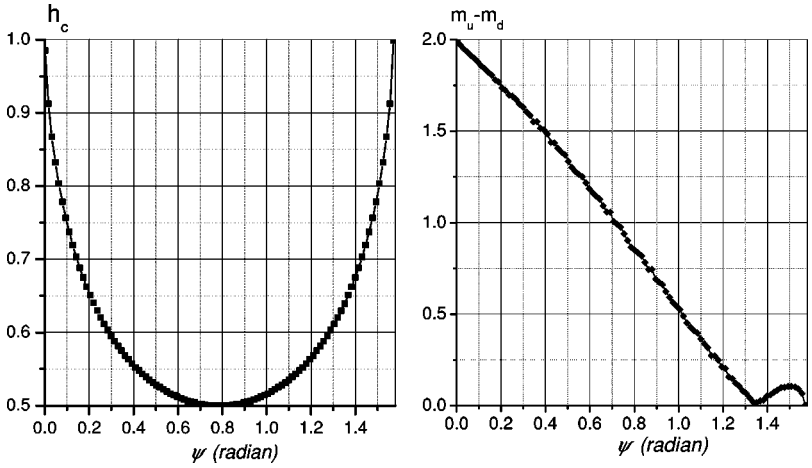

FIG. 2. One-spin problem. Left: critical field as function of ψ. Right: height of magnetization jump as function of ψ.

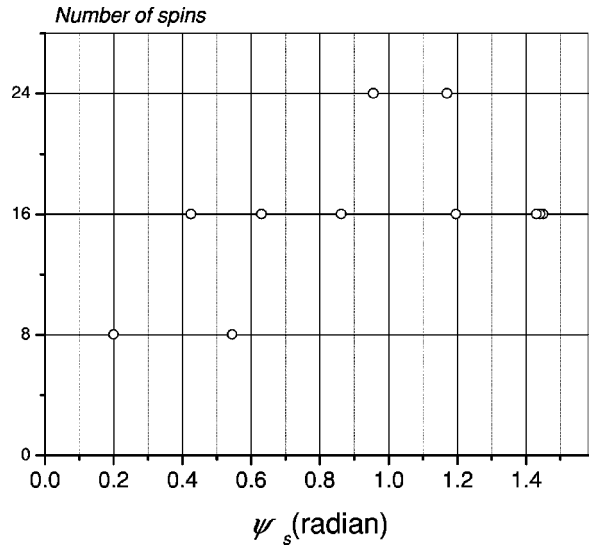

FIG. 3. Distribution of surface anisotropy axes versus the azimuthal angle ψ_s for a spherical particle with $D=10$ ($\mathcal{N}=360$: 176 surface spins and 184 core spins).

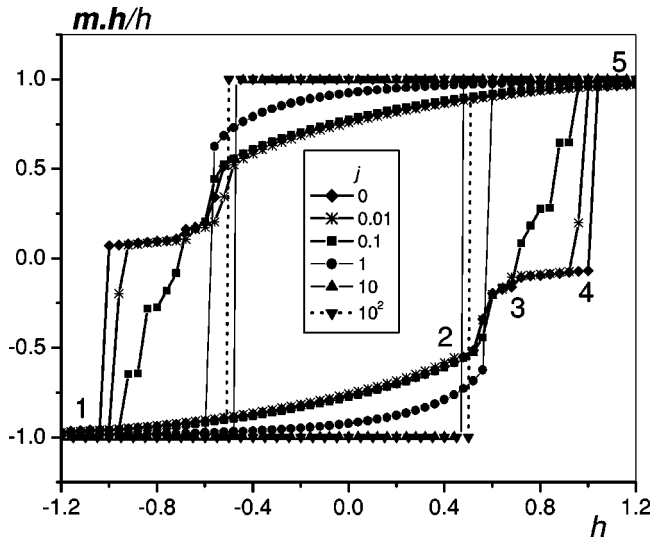

FIG. 4. Hysteresis loop, i.e., plot of the magnetization projection on the field direction as a function of the (reduced) field h, for $\psi=0$, $k_s=1$ and different values of j. $\mathcal{N}=360$.

with crossing branches as exhibited by the hysteresis for $\psi=85°$ in Fig. 1 (left), see Ref. 12 for a discussion of this issue.

IV. SPHERICAL PARTICLES: RESULTS AND DISCUSSION

Here we consider a single-domain spherical particle of simple cubic (sc) structure with uniaxial anisotropy in the core and anisotropy constant K_c, and radial anisotropy on the surface with constant K_s. Our main goal here is to investigate the influence of surface anisotropy, both in direction and strength, on the hysteresis loop and SW astroid. However, we will also study the effect of exchange coupling and particle's size. Again for later reference, we plot in Fig. 3 the distribution of surface anisotropy axes of the spherical particle as a function of the azimuthal angle ψ_s between a surface spin easy axis and applied field.

A. Effect of the exchange coupling j

Now we study the effect of exchange coupling on the hysteresis loop of a spherical particle containing $\mathcal{N}=360$ spins (176 surface spins and 184 core spins). We first consider the case in which the anisotropy constants in the core and on the surface are equal, i.e., $k_s=1.0$, and the magnetic field applied along the easy axis of the core spins, so as to investigate the influence of radial direction of surface anisotropy. For $j \ll 1$, i.e., $j=0,0.01$, we can see along portion 1–2 in Fig. 4 a progressive decrease (in absolute value) of the magnetization, which is due to the alignment of surface spins, since as the field direction is along the core easy axis the core spins have a rectangular cycle and the jump is at $h=1.0$.

Next, along portion 2–3 we can see two jumps. Indeed, according to the distribution of surface easy axes in Fig. 3, and the critical field as a function of ψ in Fig. 2 (left), those surface spins with ψ_s between 0.6 and 1.0 are responsible for the first jump, and those with ψ_s between 0.4 and 0.6 or 1.0 and 1.2 are responsible for the second jump. Next, along portion 3–4 we have successive small jumps and thereby a slight decrease of the magnetization. The origin of these small jumps resides in two contributions. One contribution comes from those surface spins whose easy axis makes an angle around 0.2 with the field. Even though the corresponding height of jump is large (see Fig. 2, right), their number is rather small (see Fig. 3) thus rendering a small contribution to the magnetization. The other contribution is due to surface spins with an angle $\psi_s \simeq 1.4$, which yield a small contribution owing to the fact that the height of the corresponding jump is very small (see Fig. 2, $\psi_s > 1.2$), even though their number is relatively large. On the last portion of the lower branch of the hysteresis in Fig. 4, we see another big jump, which is due to the switching of core spins at the field $h_c = 1.0$. At last, there is a slow increase of magnetization due to a final adjustment of surface spins along the field direction. In the present case, the surface fully switches before the core (see Fig. 5).

For $j=0.1$, we see that the surface behavior remains almost the same as in the previous cases, whereas the core spins now switch clusterwise as can be seen in the fourth picture of Fig. 5. Indeed, regarding the exchange field as a small perturbation of the applied magnetic field, it is clear that the core spins located near the surface are subject to an effective field whose direction is slightly deviated from their easy axis, i.e., the corresponding angle ψ is slightly different from zero. Now, in Fig. 2 (left) we can see that this little deviation in ψ produces an important change in the switching field. On the contrary, we find that this effect is almost absent in what concerns the jumping field of surface spins, as can be seen along portion 2–3 in Fig. 4 upon comparing the loops for $j=0,0.01$ and $j=0.1$. Indeed, the surface spins responsible for these jumps have their easy axes at an angle $0.6 < \psi_s < 1.0$, and hence the change in the corresponding critical field is very small (see Fig. 2 left). In Fig. 4 we

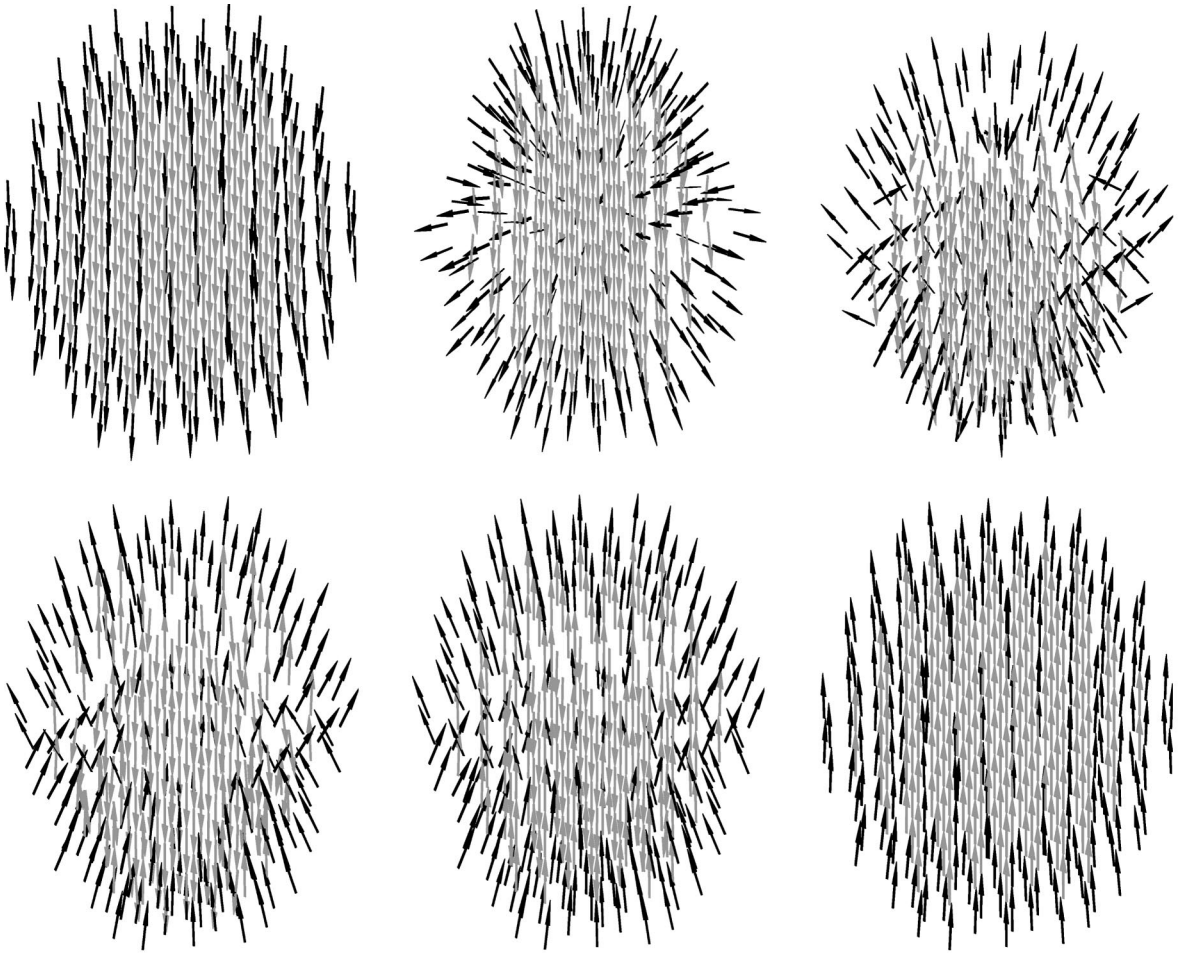

FIG. 5. Magnetic structure for $j=0.1, k_s=1$ for the field values $h=-4.0,0,0.64,0.8,0.88,4$ which correspond to the saturation states and different switching fields shown in Fig. 4. These field values correspond to the pictures when starting from the upper array and moving right, down left, and then right. Obviously, gray arrows represent core spins and black arrows represent surface spins.

can also see that for $j=0.1$, i.e., when the exchange energy becomes comparable with anisotropy and Zeeman energy, there are more jumps that can be attributed to the switching of different spherical shells of spins starting from surface down to the center. This situation is sketched in Fig. 5. For example, for $h=0$ one can see that the exchange has a little influence on surface spins, as they are directed almost along their easy axes; for $h=0.64$ the surface spins show the same behavior as in the absence of exchange, but part of core spins, located near the surface, are deviated from their easy axes. At the field $h=0.8$ all these core spins have already switched.

For $j=1\sim k_s$, even that there is only one jump, the hysteresis loop is not rectangular owing to the fact that the spins rotate in a noncoherent way, as can be seen in Fig. 6. This is due to a compromise between anisotropy and exchange energies, see, for example, the picture for $h=0$. Moreover, even a small number of neighbors lying in the core produces a large effect via exchange on the behavior of a surface spin.

For much larger values of j the spins are tightly coupled and move together, and the corresponding (numerically obtained) critical field h_c coincides with the (analytical) expression obtained in the limit $J\to\infty$, i.e., $h_c=N_c/\mathcal{N}$, where N_c is the number of core spins. This expression for h_c has been obtained by summing over the direction of surface easy axes which results in a constant surface energy contribution proportional to k_s. Hence, due to spherical symmetry, the surface anisotropy constant does not enter the final expression of h_c.

Now we consider the case of larger values of k_s, e.g., $k_s=10$, so as to investigate the influence of surface anisotropy both in direction and strength. The results are presented in Fig. 7 (left).

Here, a notable difference with respect to the previous case, $k_s=1$, is the fact that the core now switches before the surface and at higher fields. Moreover, there appear more jumps which may be attributed to the switching of various clusters of surface spins. Both cases show that as the ratio j/k_s decreases, the magnetization requires higher fields to saturate. This is further illustrated by Fig. 7 (right) where $k_s=10^2=j$ for a smaller particle.

Let us now summarize the ongoing discussion. We observe that considering a radial distribution for surface anisotropy, leads, even in the case of very strong exchange, to an important quantitative deviation from the classical SW model. In particular, the critical field in our model is given by

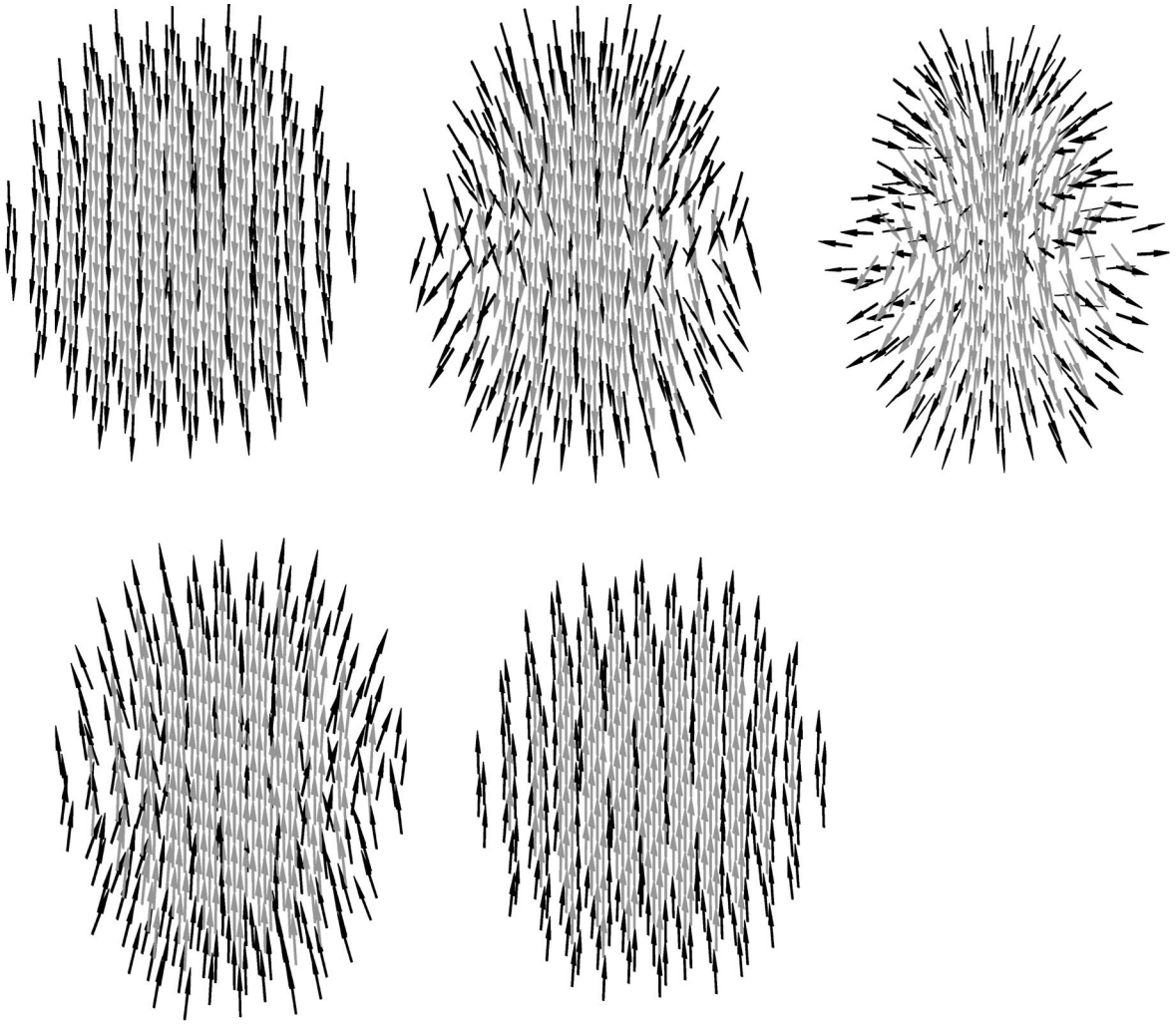

FIG. 6. Magnetic structure for $j=1, k_s=1$ for the field values $h=-4.0,0,0.56,0.6,4$ which correspond to the saturation states and different switching fields shown in Fig. 4. As in Fig. 5, gray arrows represent core spins and black arrows represent surface spins.

$$H_c^r = \frac{N_c}{\mathcal{N}} H_c^u , \tag{9}$$

where H_c^r is the critical field for a spherical particle with radial anisotropy on the surface and uniaxial in the core, H_c^u is the critical field for a spherical particle with uniaxial anisotropy for all spins. Therefore, when j and k_s are comparable, the compromise between exchange coupling, favoring a full alignment of the spins along each other, and surface anisotropy, which favors the alignment of spins along their radial easy axes, produces large deviations from the SW model. More precisely, the shape of the hysteresis loop is no longer rectangular and there appear multiple jumps. The appearance of these jumps makes it necessary to define two

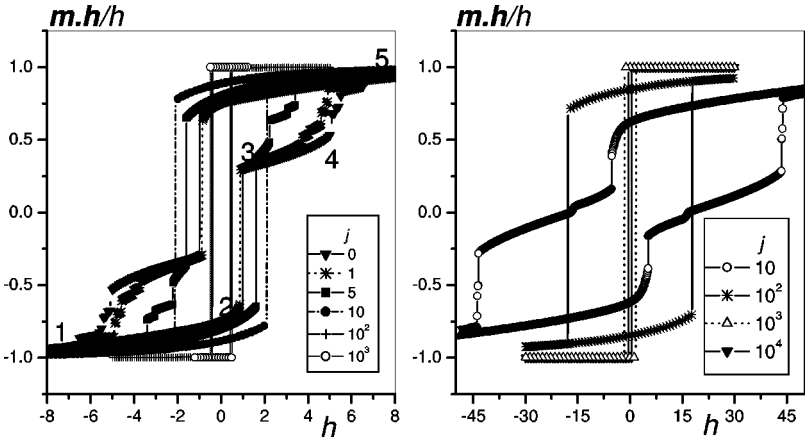

FIG. 7. Left: Hysteresis loops for $\psi=0$, $k_s=10$, and different values of j. $D=10$ ($\mathcal{N}=360$). Right: Hysteresis loops for $\psi=0$, $k_s=10^2$, and different values of j. $D=7$ ($\mathcal{N}=123$).

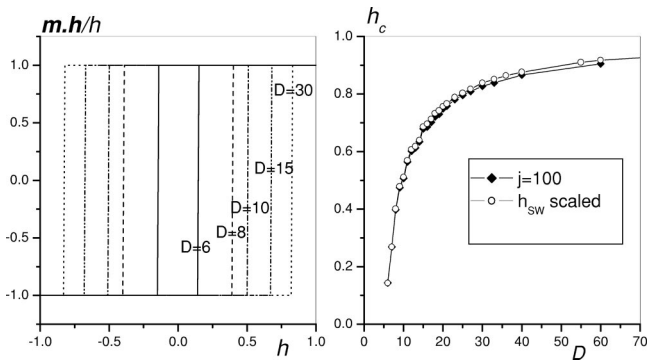

FIG. 8. Left: Hysteresis loops for $\psi=0, k_s=1, j=10^2$ for different values of the particle's diameter D. Right: (in diamonds) Switching field for the same parameters as a function of D. $h_{SW}(N_c/\mathcal{N})$ is the SW switching field multiplied by the relative number of core spins.

field values with the help of which a hysteresis loop can be characterized. A value that marks the limit of metastability, called the *critical field*, and the other value which marks the magnetization reversal, i.e., when the projection of the magnetization on the field direction changes sign, and this is why it is called the *switching field* (or still coercive field).

B. Effect of the particle's size $\mathcal{N}$

Here, we study the effect of varying the particle's size while keeping j and k_s fixed. So we use the same value of anisotropy constant for all spins and strong exchange, i.e., $k_s=1, j=10^2$, and vary the particle's diameter from 6 ($\mathcal{N}=56$) to 30 ($\mathcal{N}=12712$).

In Fig. 8 (left) are presented hysteresis cycles of a particle with different diameters when the field is along the core easy axis, and on the right the variation with the particle's diameter of the critical field[13] (in diamonds) obtained from the numerical solution of the Landau-Lifshitz equation for $j=10^2$, and (in circles) the SW critical field multiplied by the core-to-volume ratio [see Eq. (9)]. The figure on the left shows that for such a value of k_s the hysteresis loop is rectangular for all sizes, and that the critical field decreases with the particle's size. The latter fact is clearly illustrated by the figure on the right, which also shows that for $k_s=1=10^{-2}j$, all these hysteresis loops can be scaled with those

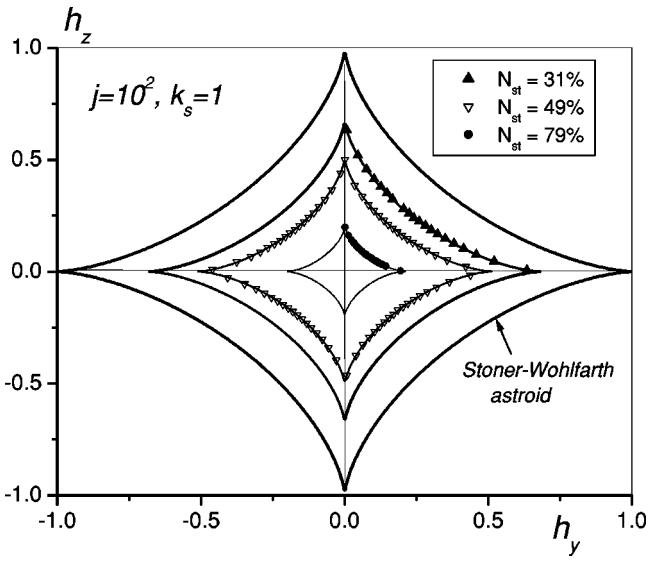

FIG. 9. Astroid for $k_s=1, j=10^2$ for different values of the surface-to-volume ratio $N_{st}\equiv N_s/\mathcal{N}$. The lines on the astroids inside the SW one are only guides for the numerical data.

rendered by the SW model. Next, Fig. 9 shows the variation with the surface-to-volume ratio $N_{st}\equiv N_s/\mathcal{N}$ of the critical field for all angles between the core easy axis and magnetic field, this is the limit-of-metastability curve. These results show that, even in the general case of a field applied at an arbitrary angle with respect to the core easy axis, the critical field of a spherical particle with $k_s=1$ can be obtained from the SW model through a scaling with constant $N_c/\mathcal{N}$. One should also note that the astroid for all particle sizes falls inside that of SW, in accordance with Fig. 8 (right), and the larger the surface contribution the more the astroid shrinks.

Therefore for $k_s=1$ our results for the hysteresis loop and limit-of-metastability curve can be scaled with those of SW model with the scaling constant $N_c/\mathcal{N}$, which is smaller than 1 for a particle of any finite size.

Next, in Fig. 10 (left) we present the hysteresis loop in the case where the surface anisotropy constant k_s equals the exchange coupling and the field is applied along the core easy axis, and in Fig. 10 (right) the switching field[14] as a function of the particle's diameter D. There are two new features in comparison with the previous case of $k_s=1$: the values of

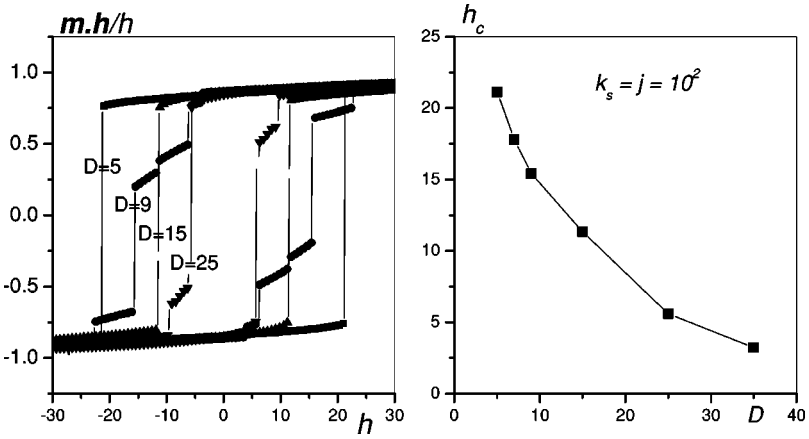

FIG. 10. Left: Hysteresis cycle for $\psi=0$, $j=k_s=10^2$, and different values of the particle's diameter D. Right: Switching field as a function of N for the same parameters.

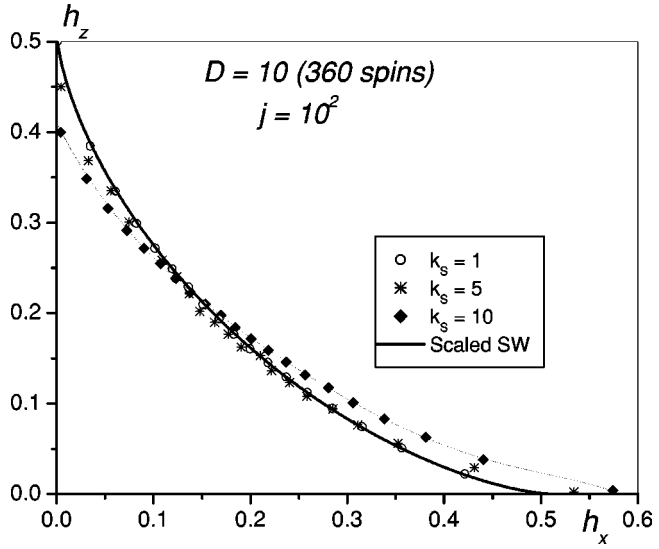

FIG. 11. Astroid for $j=10^2$, $\mathcal{N}=360$ and different values of surface anisotropy constant k_s. The full dark line is the SW astroid scaled with $N_c/\mathcal{N}$, but the dotted line is only a guide for the eye.

the switching field are much higher, and more importantly, its behavior as a function of the particle's size is opposite to that of the previous case. Indeed, here we see that this field increases when the particle's size is lowered. For such high values of k_s ($K_s \gg K_c$) surface spins are aligned along their easy axes, and because of strong exchange coupling they also drive core spins in their switching process. Thus the smaller the particle the larger the surface contribution, and the larger the field required for complete reversal of the particle's magnetization. This could explain the nonsaturation of magnetization that has been observed in, e.g., cobalt particles.[15]

C. Effect of the surface anisotropy constant k_s

Now, we fix the exchange coupling constant j, the particle's total number of spins $\mathcal{N}$, and vary the surface anisotropy constant k_s. Because K_c is in general two to three orders of magnitude smaller than J, we have investigated the effect of surface anisotropy constant in the case of $j=J/K_c=10^2$.

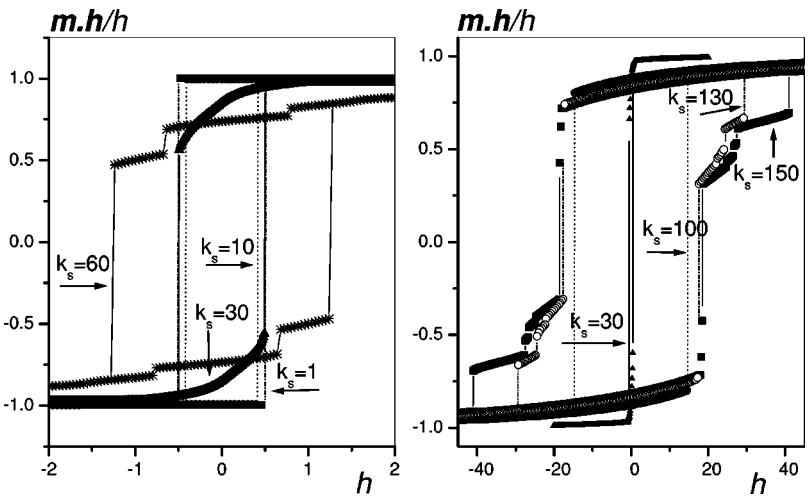

FIG. 12. Hysteresis loop for $\psi=0$, $j=10^2$, $D=10$ and different values of surface anisotropy constant k_s. These two sets of data cannot be presented as one plot because of scaling mismatch.

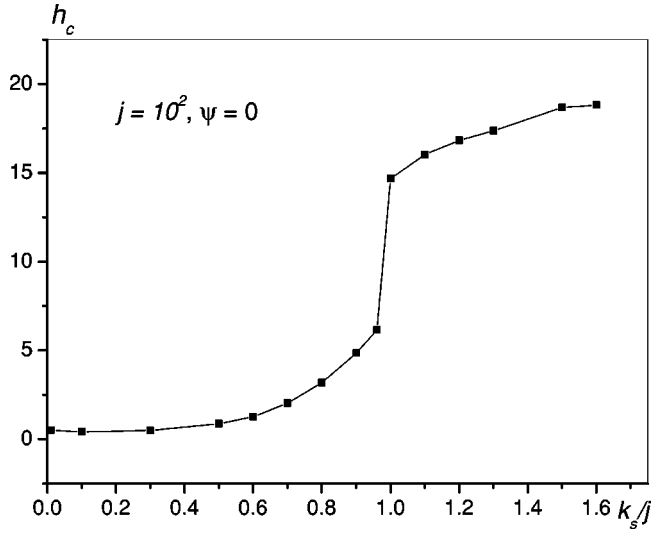

FIG. 13. Switching field versus the surface anisotropy constant for $\psi=0$, $j=10^2$, and $D=10$.

In contrast with the case $k_s=1$ and $j=10^2-10^3$ where the hysteresis loop and the limit-of-metastability curve scale with the SW ones with the same scaling constant for all angles between the applied field and core easy axis, we find that for $1<k_s<20$ the scaling constant depends on the angle ψ, as can be seen in Fig. 11. This fact explains the deformation of the SW astroid, that is a depression in the core easy direction and an enhancement in the perpendicular direction.

For larger values of k_s we have computed the hysteresis loop for $\psi=0$, $\mathcal{N}=360$, $j=10^2$. The results are given in Fig. 12.

Here, we first note that the shape of the hysteresis loop is rather different from that rendered by the SW model, since for $k_s=30$, for instance, the hysteresis loop is no longer rectangular, even that $\psi=0$. As explained earlier, this effect is due to the now more pronounced nonuniform rotation of surface spins and core spins located near the surface, and thereby that of the particle's magnetization. This nonuniform switching process causes large deviations from the SW model, and thereby no scaling with the latter is possible.

From Fig. 12, we extract and plot in Fig. 13 the switching

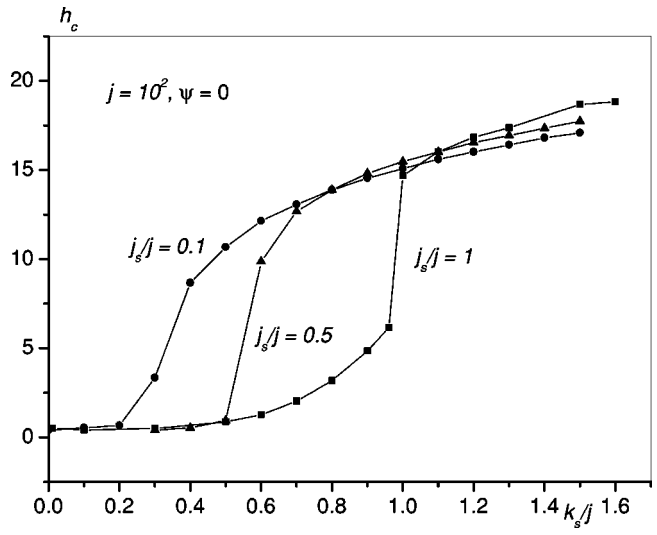

FIG. 14. Switching field versus the surface anisotropy constant for $\psi=0$, and different values of surface-to-core ratio of exchange couplings; $D=10$.

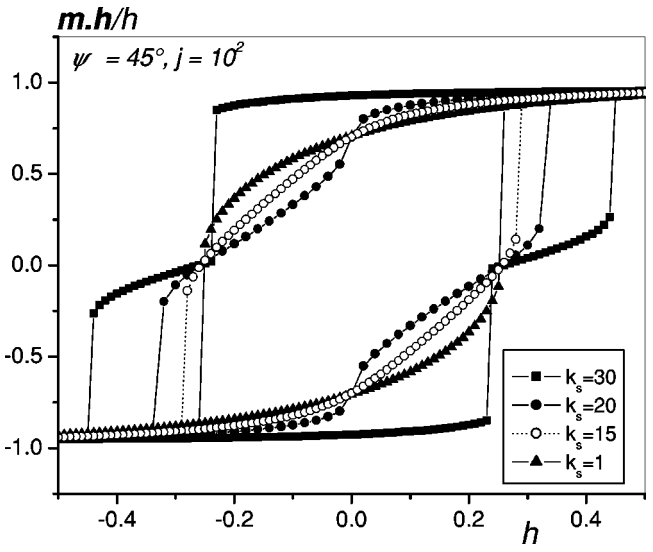

FIG. 15. Hysteresis for $\psi=45°$, $j=10^2$, $D=10$ ($\mathcal{N}=360$), and different values of surface anisotropy constant k_s.

field h_c as a function of k_s/j, denoted by $\tilde{k}_s$ in the sequel. We find that h_c first slightly decreases for $\tilde{k}_s \lesssim 0.1$ and then increases, and when $\tilde{k}_s$ approaches 1 it jumps to large values. As discussed above, for such high values of k_s surface spins are aligned along their easy axes, and because of strong exchange coupling they also drive core spins in their switching process, which then requires a very strong field to be completed. Clearly, this particular value of $\tilde{k}_s$, to be denoted by $\tilde{k}_s^c$ ($=1$, here) marks the passage from a regime where scaling with the SW results is possible (either with a ψ-dependent or independent constant) to the second regime where this scaling is no longer possible because of completely different switching processes.

Now we present additional data which show that the "critical value" $\tilde{k}_s^c$ introduced above depends on (at least) two parameters. These are the surface-to-core ratio of exchange coupling j_s/j and the angle ψ at which the field is applied with respect to the core easy axis.

Let us first discuss the effect of (intra)surface exchange coupling. In real materials such as maghemite, it was argued in Ref. 1 on account of Mössbauer spectroscopy that $j_s/j < 1$. In Fig. 14 we have plotted the results for h_c obtained with surface exchange coupling $j_s \equiv J_s/K_c$ smaller than j, i.e., core-core and core-surface couplings. First, we see that the "critical" value $\tilde{k}_s^c$ of $\tilde{k}_s$ separating the two regimes discussed above decreases with the ratio j_s/j. This is a consequence of the fact that when $j_s/j<1$, surface spins align more easily along their (radial) anisotropy axes since now they experience a weaker effective field. We also note that the jump becomes smoother. Next, if we consider the curve $j_s/j=1$ together with any other curve with $k_s/j<1$, we see that when $\tilde{k}_s<1$ the switching field is larger for $j_s<j$ than for $j_s=j$, and the opposite holds when $\tilde{k}_s>1$.

To understand this result, let us imagine a particle containing (at least) two groups of surface spins, a group 1 with exchange coupling $j_s=j$ and group 2 with $j_s<j$. When $\tilde{k}_s^2 < \tilde{k}_s < \tilde{k}_s^1$, $\tilde{k}_s^i$ being the critical value of $\tilde{k}_s$ for group i, the spins in group 1 are of SW type, while those of group 2 are of non-SW type, in the sense that they switch in a coherent way or clusterwise, respectively. Hence, as demonstrated earlier, the reversal of spins in group 2 always requires a larger switching field. On the other hand, when k_s exceeds the largest exchange coupling in the particle, i.e., j, the switching field of the whole particle decreases with j_s/j. Now the spins of both groups are of non-SW type, and their switching operates clusterwise, but obviously the latter requires a higher applied field for group 1 than for group 2.

Next, a similar effect is obtained when the field is applied at an arbitrary angle with respect to the core easy axis, as is the case for instance in an assembly of nanoparticles. Here, we consider the case of $\psi=\pi/4$. We find that there appear multiple large jumps at a smaller value of $\tilde{k}_s$ (~ 0.2), as can be seen in Fig. 15.

For an order of magnitude estimate of K_s and the critical (or saturation) field, consider a 4-nm cobalt particle of fcc crystal structure, for which the lattice spacing is $a=3.554$ Å, and there are four cobalt atoms per unit cell. The (bulk) magnetocrystalline anisotropy is $K_c \simeq 3 \times 10^{-17}$ erg/spin or 2.7×10^6 erg/cm^3, and the saturation magnetization is $M_s \simeq 1422$ emu/cm^3. The critical field is given by $H_c=(2K_c/M_s)h_c$. For $\psi=0$, $\tilde{k}_s^c=1$ and $h_c=15$, so $H_c \simeq 6$ T. On the other hand, $\tilde{k}_s^c=1$ means that the effective exchange field experienced by a spin on the surface is of the order of the anisotropy field, i.e., $zSJ/2 \sim 2K_s$. Then using $J \simeq 8$ meV we get $K_s \simeq 5.22\times 10^{-14}$ erg/spin, or using the area per surface spin (approximately $a^2/8$), $K_s \simeq 5$ erg/cm^2. For the case of $\psi=\pi/4$, $\tilde{k}_s^c \simeq 0.2$ and $h_c \simeq 0.3$, which leads to $H_c \simeq 0.1$ T and $K_s \simeq 1.2\times 10^{-14}$ erg/spin or 1.2 erg/cm^2.

V. CONCLUSION

Our model of a spherical particle with uniaxial anisotropy in the core and radial anisotropy on the surface leads to

mainly two pertinent regions for the surface anisotropy constant k_s, with $k_s > 1$ ($K_s > K_c$):

For small values of this parameter, e.g., $k_s/j \sim 0.01$, our model renders hysteresis loops and limit-of-metastability curves that scale with the SW results for all values of the angle ψ between the core easy axis and the applied field, the scaling constant being $N_c/\mathcal{N}$, which is smaller than 1 for a particle of any finite size. On the other hand, the critical field, which coincides in the present case with the switching field, increases with the particle's size and tends to the SW critical field in very large systems, and thereby the corresponding astroid falls inside the SW astroid for all particle sizes.

For larger values of k_s/j, but $k_s/j \lesssim 0.2$, we still have the same kind of scaling but the corresponding constant depends on ψ. This is reflected by a deformation of the limit-of-metastability curve. More precisely, the latter is depressed in the core easy direction and enhanced in the perpendicular direction. However, there is still only one jump in the hysteresis loop implying that the magnetization reversal can be considered as uniform.

For much larger values of k_s/j, starting from $k_s/j \simeq 1$, there appear multiple steps in the hysteresis loop which may be associated with the switching of spin clusters. The appearance of these steps makes the calculated hysteresis loops both qualitatively and quantitatively different from those of SW model, as the magnetization reversal can no longer be considered as uniform, and one has then to define two characteristic values of the field associated with a hysteresis loop: the *critical field* and *the switching field*. In addition, in the present case, there are two more new features: the values of the switching field are much higher than in SW model, and more importantly, its behavior as a function of the particle's size is opposite to that of the previous cases. More precisely, here we find that this field increases when the particle's size is lowered. This is in agreement with the experimental observations in nanoparticles (see, e.g., Ref. 16 for cobalt particles).

Therefore, assuming radial anisotropy on the surface, we find that there is a "critical" value $(K_s/J)^c$ of the ratio K_s/J beyond which large deviations are observed with respect to the SW model in the hysteresis loop and thereby the limit-of-metastability curve, since in this case the magnetization reverses its direction in a nonuniform manner via a progressive switching of spin clusters. So, in order to deal with these features one has to resort to microscopic approaches such as the one used in this work. In fact, it is found that the critical value $(K_s/J)^c$ is even smaller for smaller surface-to-core ratios of exchange coupling and larger angles between the applied magnetic field and the core easy direction, as it is more likely in realistic materials.

In a subsequent work we apply the present method to cubo-octahedral cobalt particles with a diameter of approximately 3 nm recently studied in Ref. 17 (see also Ref. 18 for Pt particles). These are particles with fcc structure and truncated octahedrons on the surface, in which the core has a cubic anisotropy, and the surface anisotropy easy axes are believed to be along edges and facets with different constants K_s^α but whose values are uncertain at present. In our calculations we vary these parameters and study the effect of surface anisotropy on the Stoner-Wohlfarth astroid that has been experimentally measured in Ref. 17 where these anisotropy constants have been estimated from magnetic measurements. The final outcome of our calculations should give an estimation of K_s^α by comparing with these experimental results. Another related issue of particular interest to us is the fact that these fcc particles (see Ref. 17 for cobalt and Ref. 19 for iron) seem to exhibit an effective *uniaxial* anisotropy despite their cubic crystal symmetry. This work is in progress.

ACKNOWLEDGMENTS

We thank D. A. Garanin and M. Noguès for reading the manuscript and suggesting improvements. M. Dimian thanks the Laboratoire de Magnétisme et d'Optique for the hospitality extended to him during his training under the Socrates program, 1 March–31 July 2001.

*Author to whom correspondence should be addressed. Electronic address: kachkach@physique.uvsq.fr

[1] H. Kachkachi, A. Ezzir, M. Noguès, and E. Tronc, Eur. Phys. J. B **14**, 681 (2000); H. Kachkachi and D. A. Garanin, Physica A **300**, 487 (2001).

[2] E. C. Stoner and E. P. Wohlfarth, Philos. Trans. R. Soc. London, Ser. A **240**, 599 (1948); IEEE Trans. Magn. **MAG-27**, 3475 (1991).

[3] D. A. Dimitrov and G. M. Wysin, Phys. Rev. B **50**, 3077 (1994).

[4] H. Kachkachi and D. A. Garanin, Eur. Phys. J. B **22**, 291 (2001).

[5] M. Dimian and H. Kachkachi, J. Appl. Phys. **91**, 7625 (2002).

[6] W. F. Brown, Jr., *Micromagnetics* (Interscience, New York, 1963); A. Aharoni, *Introduction to the Theory of Ferromagnetism* (Oxford Science Publications, New York, 1996); V. Shilov, Ph.D. thesis, University of Paris VII, December, 1999.

[7] L. Néel, J. Phys. Radium **15**, 225 (1954).

[8] D. A. Garanin and H. Kachkachi, cond-mat/0210098 (unpublished).

[9] A. I. Akhiezer, V. G. Bar'yakhtar, and S. V. Peletminskii, *Spin Waves* (North-Holland, Amsterdam, 1968), Chap. 1.

[10] A. Hahn, Phys. Rev. B **1**, 3133 (1970).

[11] It is sufficient to consider such a small particle, since for a strong exchange coupling and all easy axes along the same direction z the result would be the same for a large particle, but then the calculation of the SW astroid is much more time consuming.

[12] F. B. Hagedorn, J. Appl. Phys. **38**, 263 (1967); Al. Stancu, IEEE Trans. Magn. **33**, 2573 (1997).

[13] For $k_s = 1$, there is only one jump in the hysteresis loop as can be seen in Fig. 8 (left). Hence the critical field coincides with the switching field.

[14] This is different from the critical field in the present case of $k_s = 10^2$.

[15] M. Respaud, J. M. Broto, H. Rakoto, A. R. Fert, L. Thomas, B. Barbara, M. Verelst, E. Snoeck, P. Lecante, A. Mosset, J. Osuna, T. Ould Ely, C. Amiens, and B. Chaudret, Phys. Rev. B **57**, 2925 (1998).

[16] J. P. Chen, C. M. Sorensen, K. J. Klabunde, and G. C. Hadjipanayis, Phys. Rev. B **51**, 11 527 (1995).
[17] M. Jamet, W. Wernsdorfer, C. Thirion, D. Mailly, V. Dupuis, P. Mélinon, and A. Pérez, Phys. Rev. Lett. **86**, 4676 (2001).
[18] D. R. Rolison, in *Nanomaterials: Synthesis, Properties, and Applications*, edited by A. S. Edelstein and R. C. Cammarata (Institute of Physics, Bristol, 1998), p. 305.
[19] C. Chen, O. Kitakami, and Y. Shimada, J. Appl. Phys. **84**, 2184 (1998); T. Ibusuki, S. Kojima, O. Kitakami, and Y. Shimada, IEEE Trans. Magn. (to be published).